



*Fermi National Accelerator Laboratory
P.O. Box 500 · Batavia, Illinois · 60510*

*TD-99-054
10/29/1999*

*PRELIMINARY QUENCH-PROTECTION CALCULATIONS
FOR THE 1st FERMILAB COMMON COIL REACT AND
WIND Nb₃SN HIGH FIELD DIPOLE MAGNET MODEL*

P. Bauer

Abstract:

In the R&D effort toward a post-LHC, 100 TeV hadron collider Fermilab develops a prototype for a 10-12 T block-type dipole magnet operating at 4.5 K using Nb₃Sn superconductor with the React and Wind technology. One of the key-issues in the design of block-type high field accelerator magnets is quench protection. The following note presents some calculations of the magnitudes relevant to quench protection for some of the possible magnet design options. Different magnet design options are discussed from the quench protection standpoint. A basic protection scheme is proposed for the first common coil React and Wind Nb₃Sn high field dipole models. The formalism used throughout this work has been checked with experimental results from the LHC IR-quadrupole program. The results of the comparison as well as the details of the model are reported in another note (TD 99-045).

1) MAGNET DESIGN

The following resumes the basic parameters, relevant for a quench protection calculation, for 2 basic magnet design options: one using a cable made from 0.5 mm - diameter strands, and the second made from 0.7 mm diameter strands. Some of the parameters differ for a short and a long model. The differences are motivated by the availability of conductor material: short models will be made from material which is already available, whereas the long model design relies on an increased current carrying capacity of future material ⁽¹⁾. Secondly, long models have higher inductance and design modifications are necessary to reduce voltages during a quench. Both magnets are 2-layer hybrid designs (using NbTi in the outer layer), the bore diameter is 30 mm in both cases.

1.1) 0.5 mm Strand Design:

The cross-section of the conductor array around one aperture is shown in **Error! Not a valid link..** Its basic properties are indicated in *Table 1*. This magnet cross-section is based on a cable made from thin strands (0.5 mm diameter) aiming at cables being less sensitive to bending after reaction⁽²⁾.

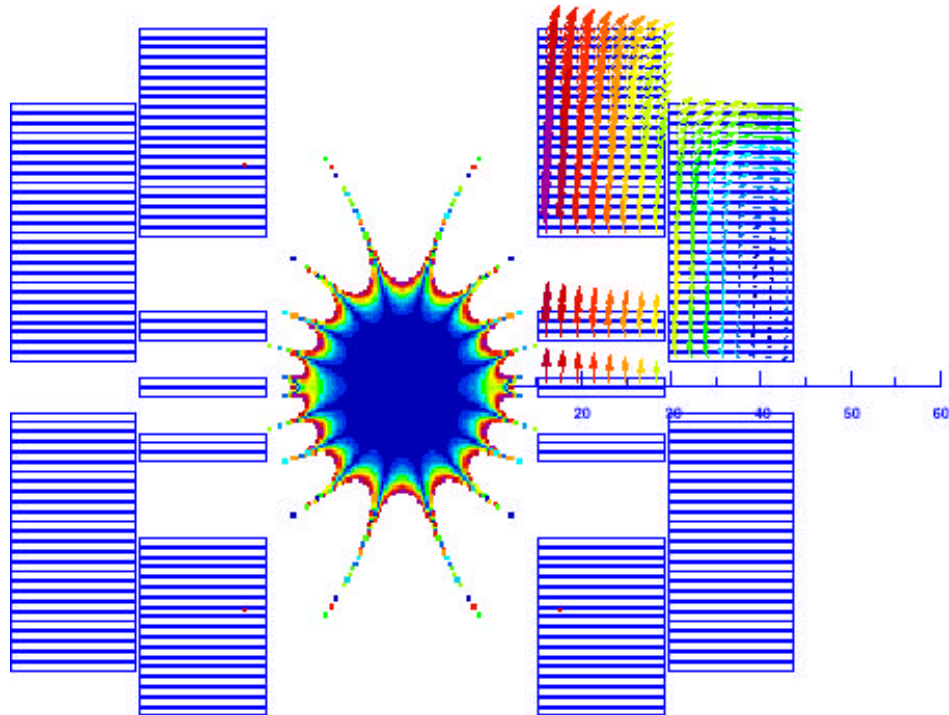


Figure 1: Roxie calculation of magnetic field in common coil racetrack coil, without iron yoke effect, 14mm wide / 1mm thick cable

¹ G. Sabbi et al., "Conceptual Design of a Common Coil Dipole for VLHC", MT 16, Jacksonville, 1999

² G. Ambrosio et al., Study of the React and Wind Technique for a Nb₃Sn Common Coil Dipole", MT 16, Jacksonville, 1999

Short sample limit bore field	11.76 T
Bath temperature	4.5 K
Peak magnetic field in inner layer	12.38 T
Peak magnetic field in outer layer	7.06 T
Short sample limit current	10850 A
Length (short)/long	(1 m) / 10 m
Spacing of upper and lower bores	262 mm
Superconductor in inner layer (short)/long	0.5 mm Nb ₃ Sn/Cu, Cu/Sc=(0.85) / 1.5 56 strands, 14 mm wide, 0.9 mm thick
Superconductor in outer layer (short) / long	0.5 mm NbTi/Cu, CuSc=(0.8) / 1.2 , 56 strands, 14 mm wide, 0.9 mm thick
Quench propagation velocities	inner layer: 10 m/s; outer layer: 30 m/s
Number of turns per coil	inner: 50, outer: 52
self-inductance of magnet / total # of turns	8.29 mH/m / 204
StoredEnergy @ short-sample-limit	0.49 MJ/m
Cu-current density in inner layer (short)/long	(2.2 kA/mm ²) / 1.65 kA/mm ²

Table 1: Characteristics of the common coil racetrack high field dipole prototype magnet, 1st design iteration.

1.2) 0.7 mm Strand Design

The second design iteration step aimed at a decrease of the inductances in the magnet by using thicker cables made from 0.7 mm strands.

Short sample limit bore field	11.03 T
Bath temperature	4.5 K
Peak magnetic field in inner layer	11.79 T
Peak magnetic field in outer layer	6.50 T
Short sample limit current (short) / long	(15000 A) / 15340 A
Length (short) / long	(1 m) / 10 m
Spacing of upper and lower bores	262 mm
Superconductor in inner layer (short) / long	0.7 mm Nb ₃ Sn/Cu, Cu/Sc=(0.85) / 1.5, 40 strands, 15 mm wide, 1.35 mm thick
Superconductor in outer layer (short) / long	0.808 mm NbTi/Cu, CuSc=(1.3) / 1.18, 38 strands, 15.4 mm wide, 1.4 mm thick
Quench propagation velocities	inner layer: 10 m/s; outer layer: 30 m/s
Number of turns per coil	inner: 36, outer: 38
Self-inductance of magnet / total # of turns	4.29 mH/m / 148
StoredEnergy @ short-sample-limit	0.42 MJ/m
Current density in Cu, inner layer (short)/long	(1.9 kA/mm ²) / 1.5 kA/mm ²

Table 2: Characteristics of the common coil racetrack high field dipole prototype magnet, 2nd design iteration.

2) HEATER DESIGN

Using today's standard protection heater technology ⁽³⁾, a basic heater consists of a 25µm stainless steel foil cut into the shape of a 2 x 2 m long, 15 mm wide racetrack embedded between 2 layers of 25 µm thick polyimide foil (Kapton[®]). The 4m long 15mm wide track has a low temperature resistance of ~5 Ω. The heater delay time (= heat diffusion time through the polyimide insulation layers on the heater (25µm) and the superconducting cable (here 100µm)) is assumed to be ~ 30 ms⁽³⁾. The heater current is supplied by a 10 mF, 1 kV peak voltage capacitor unit. The time constant of such a unit is approximately 50 ms, which is an upper limit for the time constant of a typical high field superconducting magnet protection heater (the quench process usually ends within 100 ms). There are ways to enhance the performance of such a heater unit. Its active surface can be doubled by connecting 2 heaters in series and 2 capacitor units in parallel (connecting the middle point between the capacitor banks to ground to keep the voltage to ground to less than 1 kV). Its length can be extended by covering selected areas of the resistive strip with a thin Cu coating, as it is actually proposed for the LHC dipole quench heaters⁽⁴⁾. Such a heater applied to a common coil racetrack dipole magnet, as described in chapter 1, results in the scheme shown in **Error! Not a valid link..** Note that the heater does not stay in the plane of the coil module, but crosses over to the other side of the beam tube. By covering all the coils with one heater the peak to ground voltages can be reduced in case one of the heaters fails. Note as well, that the heaters are located between inner and outer layer of the magnet. In the best case they can simultaneously heat both layers. Given a heater of the LHC type the number of conductors covered by such a heater has to be determined from its active surface (600 cm²). The heater is most efficiently used when it is clamped between the layers and if it covers only conductors and no wedges. The total power delivered by the heater system has to be sufficient to quench the conductor. The heaters described here deliver 2.5 kJ (calculation based on a peak voltage of 700 V and a 10 mF capacitance). Assuming a 50 ms time during which the heater generates power and the above mentioned active heater surface this heater produces ~ 80 W/cm². The enthalpy required to raise the temperature of an LHC IR-quadrupole outer layer cable to its critical temperature (here ~8K) is ~ 0.4 J/m. With the heater power distributed over 20 conductors on a length of ~ 6 m, the required energy becomes ~ 50 J. However, a sufficient heat margin should be included to account for the heat absorbed in the insulation and helium. A similar calculation for a cable consisting of Nb₃Sn/Cu (60 strands, strand diameter: 0.5 mm, Cu/Sc-ratio=1) yields an energy requirement of ~ 7 J/m. The energy to quench a Nb₃Sn-superconductor is higher because its critical temperature (~ 20 K) is more than twice as high as that of NbTi. However, it seems that the high margin in the NbTi heater design should make a seamless transfer of these heaters to Nb₃Sn magnets possible.

³ "Quench Protection Studies of Short Model High Gradient Quadrupoles", R. Bossert et al., *IEEE Transactions on Applied Superconductivity*, Vol. 9, No.2, June 1999;

⁴ "Quench Process and Protection of LHC Dipole Magnets", F. Rodriguez-Mateos et al., *LHC Project Note 184*, CERN, June 1999;

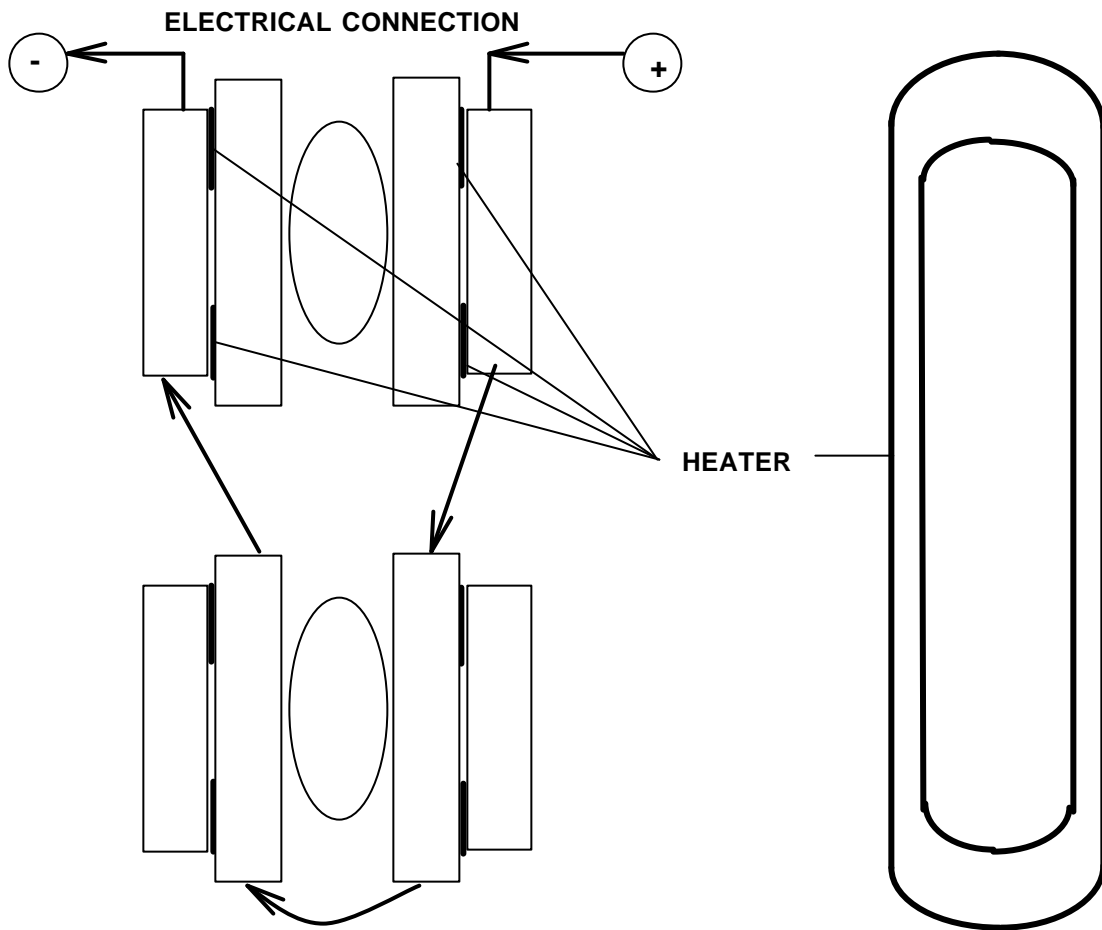


Figure 2: Schematic of heater; To reduce thermal and electrical unbalance in the magnet when a heater fails, the heaters cross over to the coils on the other side of the aperture. The sketch shows as well the electrical connections between the coils.

3) QUENCH CALCULATION MODEL

A model used to simulate the quench process is described in detail in TD 99-045.

3.1) Nb_3Sn

The material-parameters used in the calculation of the specific heat of the Nb_3Sn superconductor are given in *Table 3* (together with the material data for Cu and NbTi).

Parameter	Unit	NbTi _(46.5%)	Nb ₃ Sn	OFHC Copper
γ	[J/K ² /kg]	0.1450	0.183	0.011
β	[J/K ⁴ /kg]	0.0023	0.0042	0.000744
ρ	[kg/m ³]	6000	5400	8960
c_{p300}	[J/K/m ³]	$2.304 \cdot 10^6$	$1.415 \cdot 10^6$	$3.454 \cdot 10^6$
B_0	[T]	14.5	20	-
T_{sc0}	[K]	9.09	19	-

Table 3: Specific heat material parameters from (5) for NbTi and Cu and (6), (7) for Nb₃Sn.

The normal state, high temperature, specific heat of Nb₃Sn is calculated using a different procedure (from that described in TD 99-045), the normal state c_p -parameters for Nb₃Sn are taken from a linear interpolation of experimental data⁽⁸⁾ (see appendix).

3.2) Inductance-Calculation

A general problem related to the calculation of peak voltages in the magnet during quenches is already reported in TD 99-045. The degree of accuracy of the voltage calculations is strongly linked to the degree of subdivision of the magnet for the mutual- and self-inductance calculations. The following plot resumes a comparison of coil to ground voltage computations for a high field common coil racetrack magnet similar in most respects to the design presented in 1.2) using different degrees of subdivision. It shows that the peak to ground voltage calculations converge when the magnet is modeled into 12 separate coil-parts or more (see *Figure 3*). A peak to ground voltage calculation with a maximum degree of discretization of the coil is necessary to calculate the turn to turn voltage. As a side product of these calculations the convergence of the peak to ground voltage calculations indicated above was successfully verified, thus the peak to ground voltage calculated with a discretization at the turn to turn level agreed with the results based on a subdivision into 16 parts (see *Figure 12*). Unlike the 4-16 part cases which were based on inductance calculations provided by Roxie⁽⁹⁾, the turn to turn inductance-matrix was calculated directly from the conductor-positions. The conductors were approximated as round, with a diameter equal to the cable width. Using Ampere's law the magnetic field produced by each turn is computed and by division through current converted into the mutual and self-inductance coefficients. The so found inductances are within 5% of those computed with Roxie's COILBL function.

⁵ L. Dresner, "Stability of Superconductors", Plenum Press, NY, 1995

⁶ E. Gregory, "The science and technology of superconductors", Vol.2, p.500

⁷ Zong-Ping Zhao, doctoral thesis, MIT, 1990

⁸ H. Brechna, "Superconducting Magnet Systems", Springer 1973, p. 420, data from Bubble Chamber Group Data Handbook, Cern

⁹ S. Russenschuck et al., "Integrated Design of Superconducting Accelerator Magnets – a case Study of the main Quadrupole", the European Physical Journal (Applied Physics), p.93, Jan. 1998

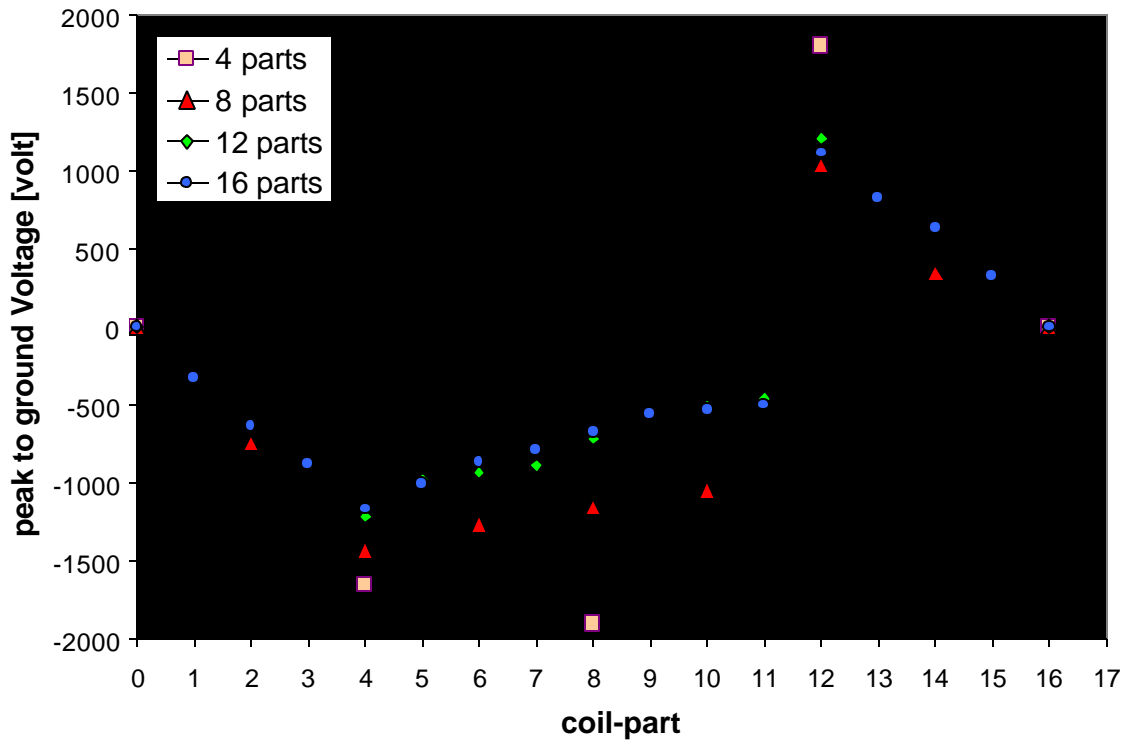


Figure 3: Comparison of peak to ground voltage calculations for different degrees of magnet subdivision (into 4-16 parts) for a 10 m long 11 T short sample bore field racetrack – common coil magnet similar to the type described in 1.2 (Quench occurs in part 12 (inner layer)).

4) THERMOMECHANIC STRESS

Nb_3Sn being a very brittle material, thermally induced stress in the conductor during a quench becomes an important issue. The following plot shows the correlation of peak temperature and axial thermal stress for the (hypothetic) case of a Nb_3Sn/Cu cable stack restrained from any expansion during a temperature rise. The stress is calculated from the modulus $E(T)$, using a linear fit between measured data at room temperature (44 GPa) and at 4.2 K (55 GPa)⁽¹⁰⁾, and a measured⁽⁷⁾ thermal expansion factor in the room temperature to 4.2 K range (0.0026).

The calculation indicates that a temperature of 300 K causes a limiting stress of 120 MPa, the thermal expansion being of the order of 0.27 %. These limits are stipulated to protect the Nb_3Sn filaments from irreversible damage due to strain. The prestrained state of the conductor due to winding after reaction (to a 0.2 – 0.3 % level) has to be taken into account in the stipulation of the thermo-mechanical strain limit.

¹⁰ D. Chichili et al., "Investigation of Cable Insulation and Thermo-Mechanical Properties of Nb_3Sn Composite", MT-16, Tallahassee Fl. 1999

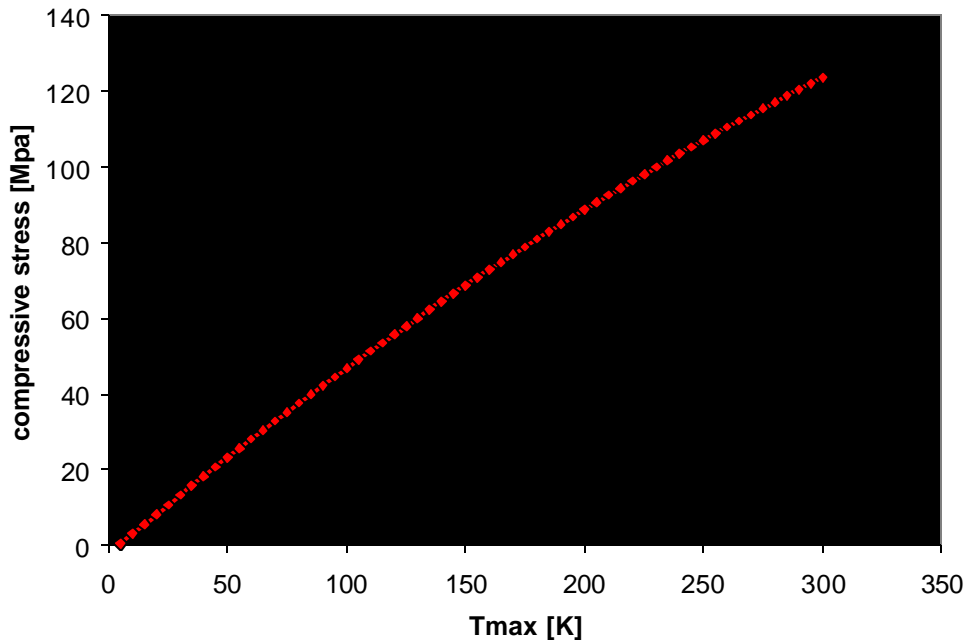


Figure 4: Axial (longitudinal) thermal stress vs. peak temperature for a $Nb_3Sn/Cu/epoxy$ cable stack restrained from any longitudinal expansion during a temperature rise.

5) QUENCH PROTECTION CALCULATIONS

Typically quench protection schemes are based on worst case scenarios. Therefore the calculations presented here usually refer to short sample limit current and peak fields. Since the peak temperatures are computed from an adiabatic model they should overestimate the real temperatures. The current decay model underestimates the current decay rate because it does not include quench-back and tranverse turn to turn quench propagation. For the same reason, and because the model does not include the dependance of the longitudinal quench propagation velocity on magnetic field, the computed peak voltage during the magnet discharge is merely a rough estimate of the voltages expected in the real case. In general the magnet-models discussed here are MIIts-limited in the inner layer. Therefore an inner layer quench usually causes a higher peak temperature than a quench in the outer layer. In what refers to peak to ground voltages the worst case scenarios would be that of heater failure causing thermal and electrical imbalances within the magnet. This particular case has not been considered here. It seems that in most cases the peak to ground voltage is independent of the quench-location (as long as the quench occurs in the inner layer). The electrical sequence of the coils plays a role in the voltage distribution - the powering scheme on which the here presented calculations are based is shown in *Figure 2*. The finer the subdivision of the coil the better the model is for the computation of the voltages within the coils and from the coils to ground. In general, a subdivision into 16 parts was used throughout the modeling, except for the turn to turn voltage calculation where the discretization was

extended to all 148 turns. The following protection scenarios were worked out separately for short and long magnet models for the reasons indicated in the introduction of part 1).

5.1) 0.5 mm Strand Cable

The first iteration design, described in 1.1), uses a cable made from thin strands (0.5 mm) aiming at stress/strain reduction in the conductor. The strand diameter is the determining magnitude for the peak strain during bending in a React&Wind approach. The disadvantage of a “thin”-cable design is its high number of turns, thus its high inductance, which makes the magnet difficult to protect. The simulation results presented in the table below are not within the stipulated temperatures and voltages. The peak to ground voltage calculation is based on a rough subdivision of the coil (into 4 parts). Therefore the results indicated in the following table overestimate the expected voltage. The only way to keep the peak temperatures below ~ 250 K in the inner layer is to massively increase (factor 2-3) the copper to superconductor ratio. In the current design the current density in the copper after a quench is 2100 A/mm^2 in the short model and 1650 A/mm^2 in the long model. Both figures are higher than the “rule of thumb” limit of $\sim 1500 \text{ A/mm}^2$. Unfortunately the design of the magnet cross-section would be totally modified by such an increase in the copper content of the conductor. In order to keep the peak-temperatures as low as possible all conductors have to be covered with heaters, resulting in an accelerated current decay. The fast current decay unfortunately drives the voltages in the long model to 3-4 times the limit (2 kV) (see *Table 4*).

Que. orig.	Heated layers	Heated turns	t_0 [ms]	Cu/Sc in	Cu/Sc out	L [mH]	T_{\max} in [K]	T_{\max} out [K]	V_{\max} [kV]	comment
in	all	all	35	0.85	0.8	8.29	470	70	< 1.7	short model, inner coil quench
out	all	all	35	0.85	0.8	8.29	100	280	< 1.2	short model, outer coil quench
in	all	all	35	1.5	1.2	83	310	70	< 7.2	long model, inner coil quench
out	all	all	35	1.5	1.2	83	100	265	< 78	long model, outer coil quench

Table 4: Simulated quench protection scenarios for the 0.5 mm strand cable common coil dipole; Parameters: number of conductors per heater per coil quenched with heater, t_0 (time after a spontaneous quench at which heater activity sets in), quench location (outer vs. inner layer), Cu/Sc inner layer, CuSc outer layer, total inductance L;

Neither the 10 m long nor the short model magnet design are satisfactory from the magnet protection point of view. However, the short model could be protected by an extraction resistor clamping the output at quench detection time. Included in the design of the short model quench protection model is a reduced heater delay time ($t_0=35$ ms). The heater delay time has a huge effect on the final temperature of the winding. It is not guaranteed that heater delay times can be kept much below 40 ms. Other ways have to be found to protect the long model. A possible solution is to reduce the total inductance by a factor 2, e.g. by driving parts of the coil separately, and to cover only half of the turns with quench heaters.

5.2) 0.7 mm Strand Cable

The second iteration design, described in 1.2), uses a cable made from thicker strands (0.7 mm). The advantage of a “thick”-cable design is the reduced number of turns, thus the reduced inductances, which makes the magnet easier to protect. In fact the cross-section iteration 2 has approximately a 2 times smaller self-inductance, and mutual inductances are reduced by a factor 4. As in 5.1 the case of a short and a long model were analysed separately. As can be seen from the following table the short model in the original design runs into high peak temperatures (>500 K) in the inner layer due to a lack of copper (copper current density at short sample limit: 2120 A/mm²). With enough margin in peak to ground voltage a reduction of the Cu/Sc ratio in the outer layer can be considered. This would reduce the peak temperatures through acceleration of the current decay (and thus raise the peak to ground voltage). Rows 2 and 4 in the following table unfortunately show that within a reasonable range of Cu/Sc ratios the effect is too small to significantly reduce the peak temperature in the inner layer. However, short models can always be protected with extraction resistors. A rough estimate shows that a dump-resistor of ~60mΩ can bring the current down to 65% of its start value within the 30 ms of the heater delay time. The resistance of the short model magnet quickly rises to ~220 mΩ during heater action. Therefore after t_0 the dump-resistor will take over ~30% of the remaining energy. The dump resistor protects the short model magnet, extracting ~ 75 % of the heat (900 V peak voltage).

Que. orig.	Heated layers	N_h	t_0 [ms]	CuSc in	CuSc out	L [mH]	T_{max} in [K]	T_{max} out [K]	V_{max} [kV]	comment
in	all	all	35	0.85	1.3	4.3	575	50	< 0.7	short model, inner coil quench
in	all	all	35	0.85	0.8	4.3	570	60	< 0.7	short model, reduced Cu/Sc in outer layer inner coil quench
out	all	all	35	0.85	1.3	4.3	170	120	< 0.35	short model, outer coil quench
out	all	all	35	0.85	0.8	4.3	160	155	< 0.33	short model, reduced Cu/Sc in outer layer outer coil quench
in	all	all	35	1.5	1.2	43	430	70	<2.5	long model, inner coil quench
in	all	all	35	1.5	1.2	43	300	60	<1.9	long model, inner coil quench*
out	all	all	35	1.5	1.2	43	155	150	< 2.2	long model, outer coil quench

Table 5: Simulated quench protection scenarios for the 0.7 mm strand cable common coil dipole at short sample limit conditions; Parameters: N_h (number of conductors per heater per coil quenched with heater), t_0 (time after a spontaneous quench at which heater activity sets in), quench location (outer vs. inner layer), Cu/Sc inner layer, CuSc outer layer, inductance L; (*..operating conditions)

The long model case stays within the stipulated limits at operating conditions (see following plots). At short sample limit the limits are slightly exceeded (see Table 5).

The following plots show the MIIts-profiles, current decay, temperature profiles and peak voltage to ground curves for the long 0.7 mm strand magnet design discussed in 1.2) at operation conditions (13.65 kA / 10T). In these simulations the quench occurs in an inner layer. Quench-heaters, covering all turns are fired and the output clamped by a low resistance.

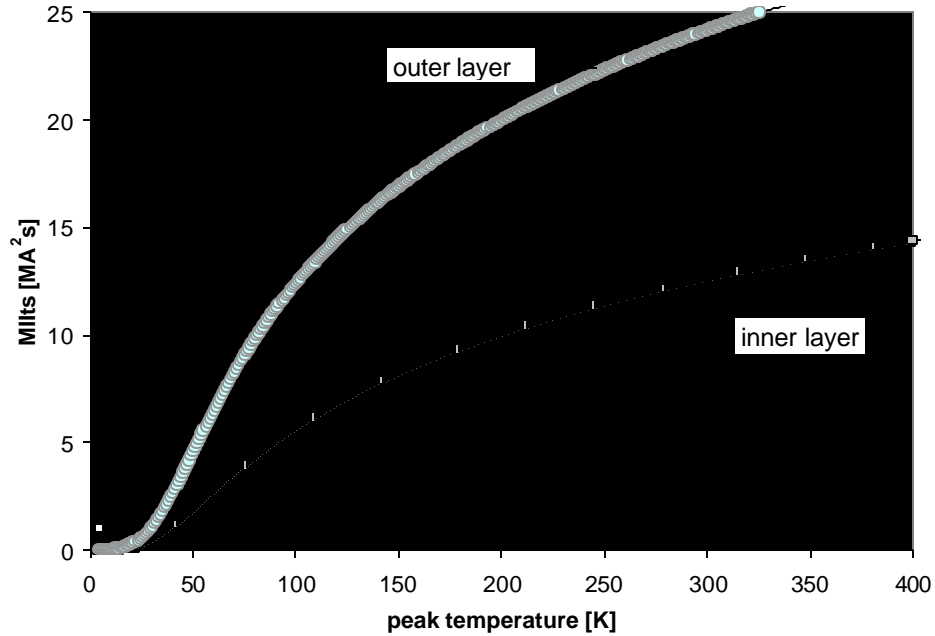


Figure 5: MIIts vs. peak temperature relation for inner and outer layer conductor for magnet design 1.2 (cables made from 0.7 mm strands).

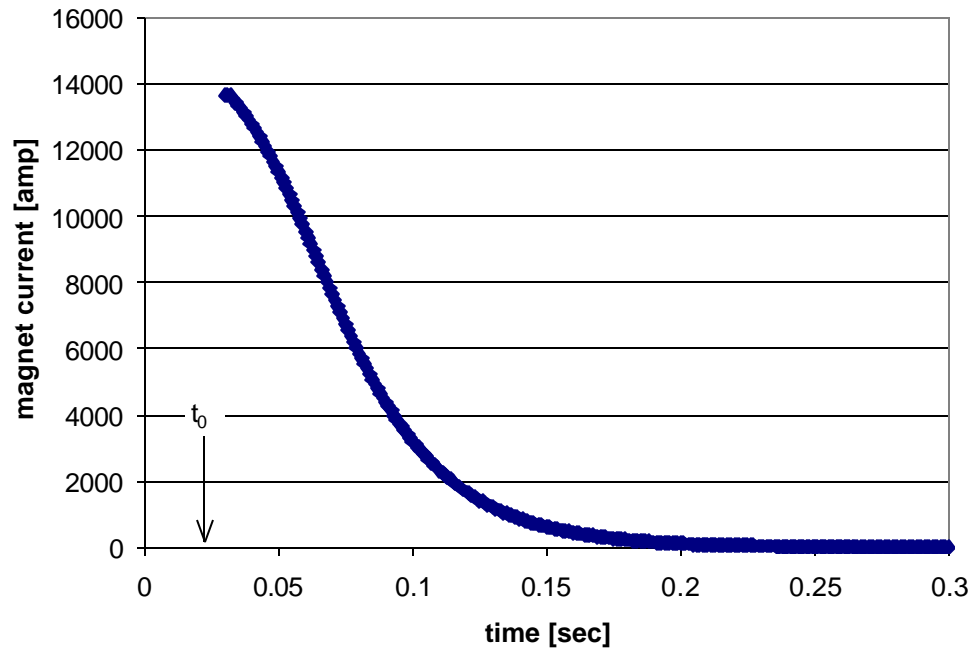


Figure 6: Current decay after quench heater firing in magnet design 1.2 at operating conditions (13.65 kA, 10 T); (cables made from 0.7 mm strands);

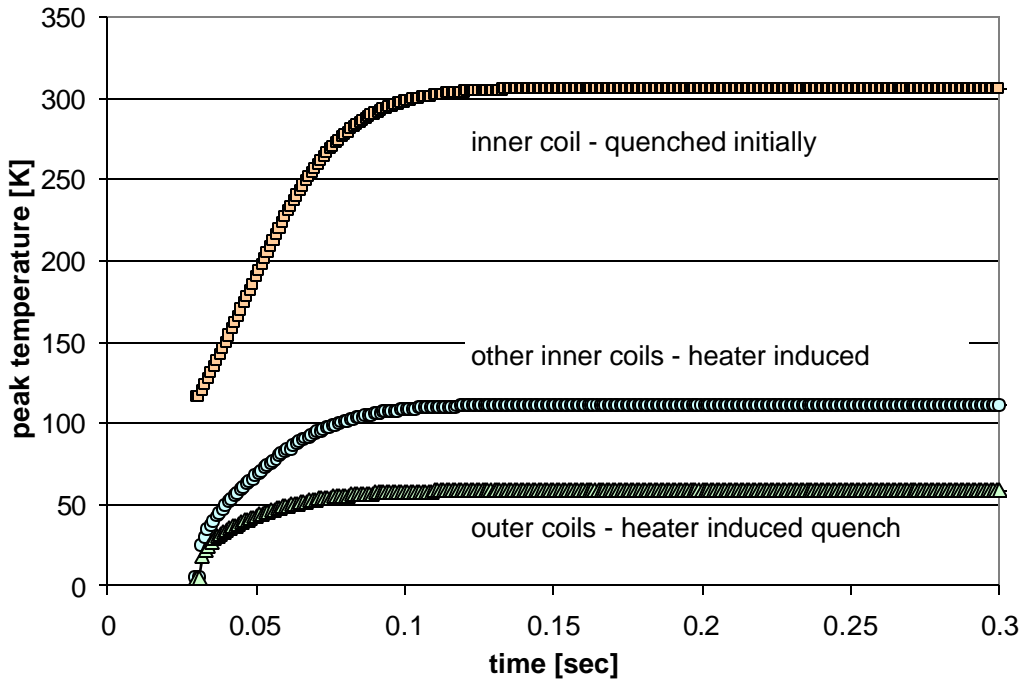


Figure 7: Temperatures in magnet design 1.2 (cables made from 0.7 mm strands) after a spontaneous quench in an inner coil and heater induced quenches in all other coils at operating conditions (13.65 kA, 10 T).

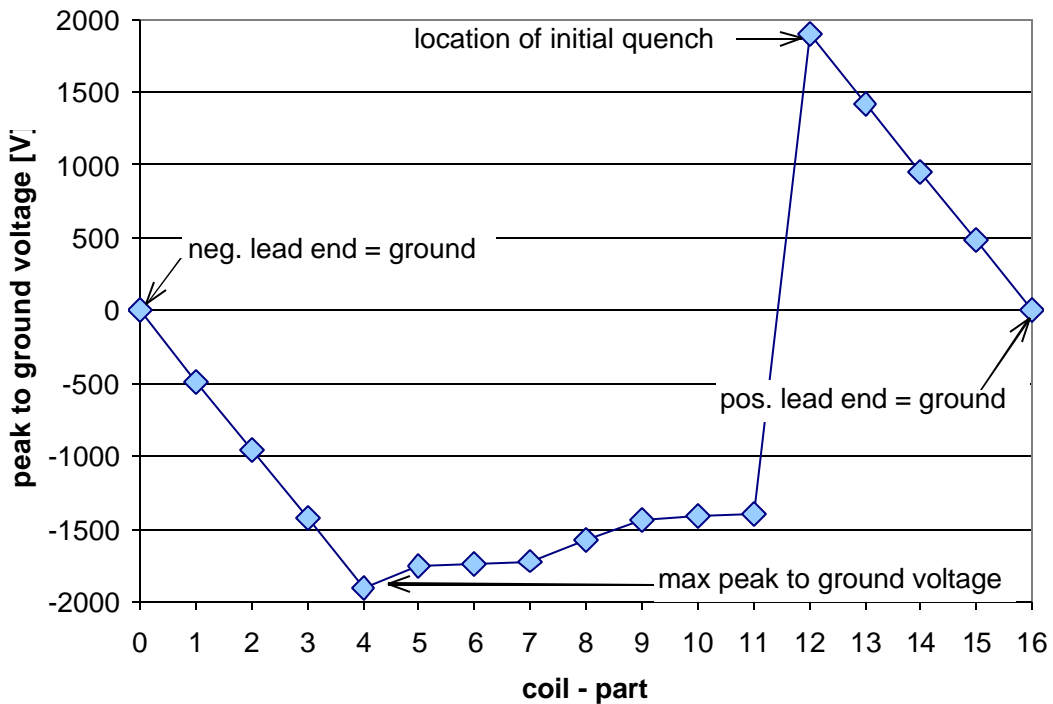


Figure 8: Peak to ground voltages during magnet discharge in the different coil-parts of magnet design 1.2 (cables made from 0.7 mm strands) after a spontaneous quench in an inner coil and heater induced quenches in all other coils at operating conditions (13.65 kA, 10 T).

The following plots show the temperatures and the computed peak to ground voltage and the turn to turn voltage of the long 0.7 mm strand magnet design discussed in 1.2) at short sample limit conditions (15.34 kA / 11.03 T).

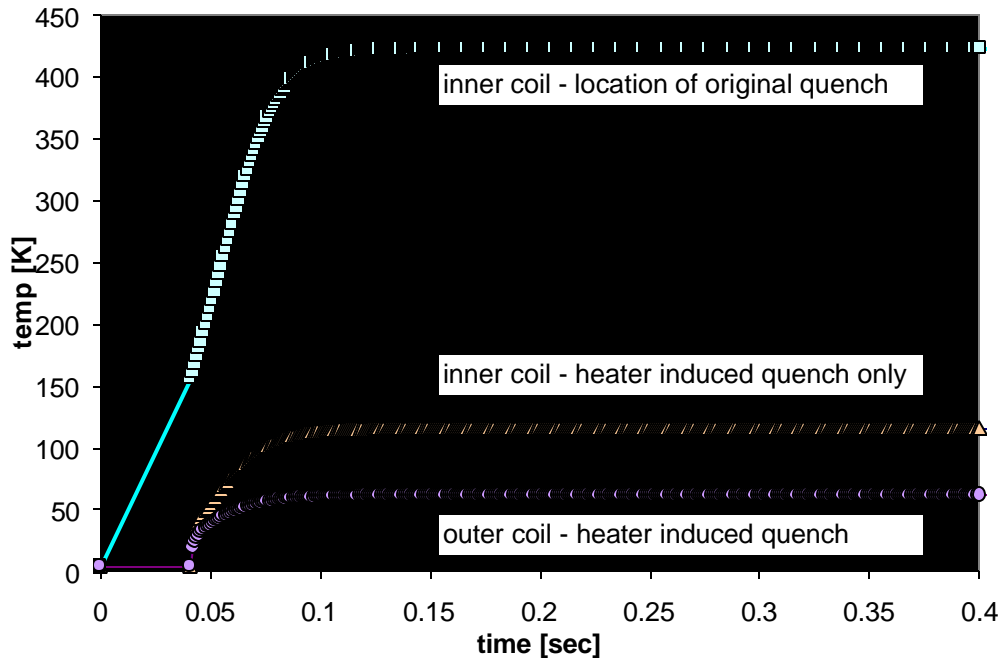


Figure 9: Peak temperatures in a 10 m long magnet described in 1.2) at short sample limit conditions (15.34 kA, 11 T). The spontaneous quench occurs in an inner layer. 75% of all turns are covered by protection heaters.

The following plots showing peak to ground and turn to turn voltage can be interpreted in the following way:

The peak to ground voltage, that is the cummulated voltage to ground along the coils at the moment of maximum resistive (and therefore maximum of inductive) voltage along the quench process, is a sum of inductive and resistive voltages. In the present case, with the quench occuring in the inner coil that is furthest away from the grounded lead, the inductive voltage is basically a linearly increasing from 0 to -10 kV along the coil. The resistive voltage roughly follows a comparable curve going to $+10$ kV. In fact the resistive voltage rises slowly in the outer layers (which are not as resistive as the inner layers) and faster in the inner layers. A strong resistive peak occurs at the conductor group, which quenched originally (and which is therefore hottest and most resistive). The overall peak voltage to ground function therefore goes to negative values in the coils where the inductive voltages dominates, whereas it has a large positive peak at the location of the original quench. The turn to turn voltage basically shows three patterns: an outer layer pattern of moderate voltage differences, an inner layer pattern showing a stronger resistive (positive) voltage component and the spike at the orgiginal quench location. The difference in turn to turn voltage within a block is caused by the fact that some conductors are not heated by protection heaters and therefore not resistive (they

show just the inductive components). The peak turn to turn voltage for the 0.7 mm strand magnet at short sample limit conditions is < 1 kV.

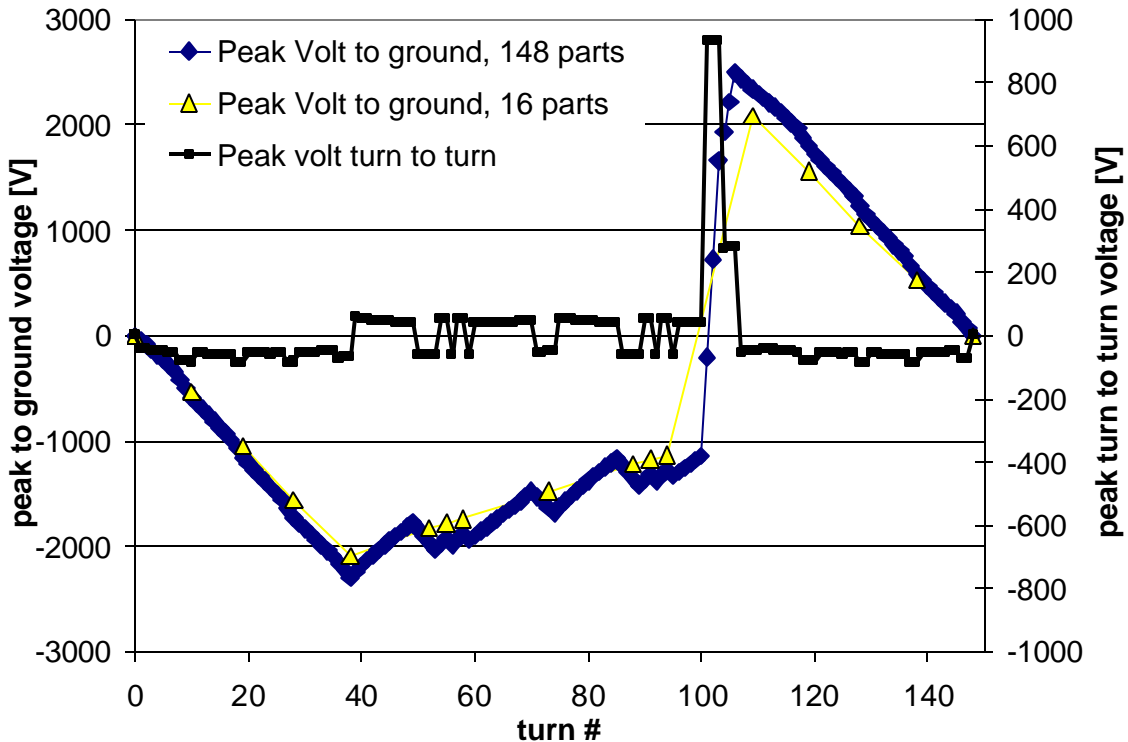


Figure 10: Peak to ground voltage and peak turn to turn voltage in a 10 m long magnet described in 1.2) at short sample limit conditions (15.34 kA, 11 T. The peak to ground voltage has been computed with different granularities of the model – 16 part subdivision and turn by turn (148 parts) subdivision.

6) CONCLUSIONS

High field superconducting magnets (here 10 – 12 T) are operating at high currents. Block-type magnets, especially without auxilliary coils, are less “conductor-efficient” and tend to have more turns than for example their $\cos\theta$ homologues. In addition the React&Winbd approach requires cables made from thin strands. A thinner and thus smaller cable raises the required number of turns to meet the demands on the bore field side. Big number of turns results in high inductance. Furthermore Nb_3Sn superconductor, which will be used in the inner layer of the first Fermilab common coil type dipole model has a smaller specific heat than NbTi, resulting in reduced MIIts budgets compared to comparable NbTi conductors. Finally, due to its brittleness, Nb_3Sn superconductor is more sensitive to temperature excursions than NbTi. All in all, the type of magnets discussed here are difficult cases from the quench protection point of view. The standard protection techniques for superconducting accelerator magnets will have to be applied at their limits in order to protect the magnets discussed here. However, the right combination of design and protection system parameters should make the task of quench protection in long, high field, common coil dipoles possible.

The analysis of the quench protection parameters for the first two design iterations for 10-11T common coil dipole model can be resumed in the following:

The design based on cables made from 0.5 mm diameter strands will demand special measures for the protection. Especially in the 10 m long model both peak temperatures and peak voltages by far exceed the thresholds. The design based on cables made from 0.7 mm diameter strands leads to peak temperatures and voltages, which exceed slightly the stipulated limits. This applies especially to the short model, which can only be operated with the additional safety provided by an extraction resistor. The 10 m long model becomes critical at short sample limit. Therefore several issues should be investigated in this case. The issues to be considered are:

- reducing the quench detection time;
- dielectric strength of the insulation (helium);
- heater geometry (how to cover all turns);
- efficiency of the heaters;

7) APPENDIX

Cp(T) data for normal state Nb₃Sn in J/K/kg:

T [K]	Cp [J/K/kg]
0	0
2	0.58
4	1.23
6	2.01
8	2.99
10	4.23
12	5.8
14	7.76
16	10.19
18	13.1
20	17.1
22	20.8
24	24.9
26	31.1
28	38.7
50	97
100	200
120	220
150	232
200	250
300	262